

ESR of Mn^{2+} in $AlCl_3$ -graphite intercalated compounds

G. Ceotto, G. E. Barberis, and C. Rettori

*Instituto de Física "Gleb Wataghin," Universidade Estadual de Campinas (UNICAMP), Caixa Postal 6165,
13 081 Campinas, São Paulo, Brazil*

(Received 21 December 1988)

Electron-spin-resonance experiments of Mn^{2+} impurities in stage-2 $AlCl_3$ -graphite intercalated compounds show the usual conduction-carrier spin resonance and a completely resolved Mn^{2+} spectrum of axial symmetry with the axial axis perpendicular to the carbon layers. The temperature dependence of the Mn^{2+} second-order crystal-field parameter and spin-lattice relaxation time are reported. The hyperfine splittings were found to be temperature independent. The observed anomalies in the linewidth of the conduction-carrier spin resonance and the intensity of the Mn^{2+} resonance at $T \approx 200$ K are interpreted in terms of a quasi-two-dimensional order-disorder phase transition experienced by the intercalant molecules at this temperature.

INTRODUCTION

Conduction-carrier spin-resonance (CCSR) experiments in graphite single crystals, highly oriented pyrolytic graphite (HOPG), and associated graphite intercalation compounds (GIC's),¹⁻⁵ has been widely used to study several properties of these highly anisotropic materials. For concentrated magnetic compounds, such as $NiCl_2$, $MnCl_2$, and $CuCl_2$ -GIC's,^{6,7} electron-spin-resonance (ESR) experiments have shown broad, anisotropic, and temperature-dependent resonances, indicating strong coupling between the magnetic ions in these compounds. Although Vaknin *et al.*^{8,9} have recently observed resonances in MoF_6 -GIC's and OsF_6 -GIC's and attributed them to single Os^{5+} and Mo^{5+} ions, respectively, little has been done in ESR of diluted magnetic impurities in GIC's. Therefore this work aims to dilute Mn^{2+} ions in $AlCl_3$ -GIC's and study the properties of these GIC's via the spin resonance of both the Mn^{2+} ions and the conduction carriers.

In this paper we report on the CCSR and the complete resolved fine and hyperfine spectra of Mn^{2+} diluted in stage-2 $AlCl_3$ -GIC's. The temperature dependence of the spectra allowed us to obtain, for Mn^{2+} , the temperature dependence of the second-order crystal-field parameter and the spin-lattice relaxation time. No temperature dependence of the hyperfine constant could be observed within the accuracy of our experiment. The temperature dependence of the CCSR was also studied simultaneously to that of the 30 ESR lines of the Mn^{2+} ions. For comparison the reference compound of pure stage-2 $AlCl_3$ -GIC was also studied.

EXPERIMENT

ESR experiments in two samples of Mn^{2+} in stage-2 $AlCl_3$ -GIC's and one of pure stage-2 $AlCl_3$ -GIC were carried out at X band in a conventional reflection spectrometer from 90 to 360 K. The temperature was controlled with a cold nitrogen gas flux system adapted to a room-

temperature TE₁₀₂ (1–100 KHz) rectangular cavity which allows the sample to be oriented with the *c* axis parallel and perpendicular to the external magnetic field (H_0), and the microwave magnetic field (H_1) always perpendicular to the *c* axis. The angular dependence of the spectra was determined at room temperature in a rotating TE₀₁₁ (100 kHz) cylindrical cavity. Except for the angular dependence of the spectra, the data were taken using a magnetic field modulation frequency of 1 kHz in order to avoid frequency modulation effects.¹⁰ Whenever the temperature dependence of the resonance intensity was analyzed, it was required that the line shape, as a function of temperature, did not present significant changes. In those cases the intensities of the resonances were calculated from the peak to peak high of the absorption derivative times the square of the linewidth.

The samples were prepared from HOPG obtained from Union Carbide Co. The intercalant material was prepared as follows. The $Al_{1-x}:Mn_x$ ($x=0.1$) alloy was obtained by arc melting the appropriate amounts of each element in an argon atmosphere. This alloy was then powdered and exposed to a Cl_2 atmosphere in a Cl_2 reactor.¹¹ The obtained chlorine compound and HOPG of an approximate size of $8 \times 3 \times 0.7$ mm³ were then sealed with a chlorine pressure of about 650 mbar in a quartz ampoule, already appropriate for the ESR and x-ray experiments. The intercalation was carried out in a two-zone furnace at $T_{HOPG} = 286^\circ C$ and $T_I = 235^\circ C$ during one day for sample No. 1 and two days for sample No. 2. The same procedure was followed in the preparation of pure stage-2 $AlCl_3$ -GIC (sample No. 0), except that pure Al powder was used in this case. (001) x-ray diffraction experiments confirmed that our samples were high-quality, pure stage-2 GIC's. The linewidth of the Mn^{2+} resonances and the low-temperature linewidth of the CCSR for fast cooling rates (see below) were found to be larger for sample No. 2 than the respective values for sample No. 1. This indicates that, probably due to the longer intercalation time, the Mn^{2+} concentration in sample No. 2 was higher.

RESULTS AND ANALYSIS

The room-temperature ESR spectra of Mn^{2+} in stage-2 $AlCl_3$ -GIC for sample No. 1 are shown in Figs. 1(a) and 1(b) for the magnetic field parallel and perpendicular to the c axis, respectively. Similar spectra were obtained for sample No. 2. The strong resonance at the center of the spectra corresponds to the CCSR with g values given in Table I. The five sets of six hyperfine lines with the appropriate fine-structure intensity line ratio 5:8:9:8:5 correspond to the transitions within the various multiplets ($S = \frac{5}{2}$, $I = \frac{5}{2}$).

Figure 2 shows, for the sample of Fig. 1, the angular dependence of the fields for resonance for one of the hyperfine lines corresponding to each multiplet. Similar data were obtained for sample No. 2, and other lines of the multiplets. This anisotropy can be described by the usual spin Hamiltonian for axial symmetry¹²

$$\hat{H} = \mu_B \mathbf{S} \cdot \vec{g} \cdot \mathbf{H}_0 + DO_2^0 + aO_4^0 + \mathbf{I} \cdot \vec{A} \cdot \mathbf{S}; \quad (1)$$

where the first term is the Zeeman interaction, the second and third terms the electric crystal-field energy, developed up to fourth order in the Stevens operators O_n^m , and the last one the hyperfine interaction. Since for Mn^{2+} the Zeeman energy is much larger than the other interactions, we chose the magnetic field direction as the quantization z axis, and calculated, up to second-order perturbation, the field for resonance of the 30 lines. The parameters in Eq. (1) were obtained by a least-squares fit of the experimental to the theoretical field for resonance of these 30 lines, for at least 20 different orientations of the magnetic field relative to the c axis. The best fit of Eq. (1) to the field for resonance of Fig. 2 gives

$$g_{\parallel} = 1.9968 \pm 0.0001; \quad g_{\perp} = 1.9996 \pm 0.0001;$$

$$D/g\mu_B = 155.1 \pm 0.2 \text{ G};$$

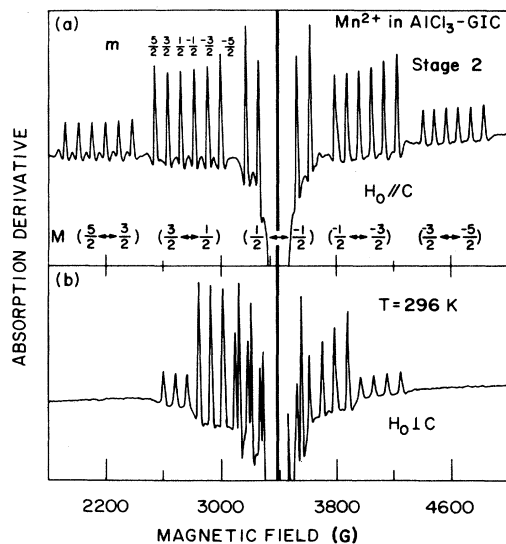


FIG. 1. ESR spectra of Mn^{2+} in stage-2 $AlCl_3$ -GIC's (a) $H_0 \parallel c$ axis; (b) $H_0 \perp c$ axis.

TABLE I. Conduction-carrier spin-resonance g values.

Sample (stage 2)	$90 \leq T \leq 295 \text{ K}$	
	$g_{\parallel} (\pm 0.0003)$	$g_{\perp} (\pm 0.0003)$
$AlCl_3$ -GIC No. 0	2.0022	2.0028
Mn: $AlCl_3$ -GIC No. 1	2.0019	2.0026
Mn: $AlCl_3$ -GIC No. 2	2.0017	2.0024

$$a/g\mu_B = (-5.2 \pm 0.4) \times 10^{-3} \text{ G};$$

$$A_{\parallel}/g\mu_B = 86.0 \pm 0.2 \text{ G}; \quad A_{\perp}/g\mu_B = 81.0 \pm 0.2 \text{ G}.$$

These results clearly indicate that the Mn^{2+} ions are located in sites of axial symmetry, with their axial axis oriented along the c axis. The relatively large values found for the components of the hyperfine tensor indicate that the covalent bonding between the chlorine and manganese atoms is relatively small.

The temperature dependence of the spectra between 90 and 360 K for $H_0 \parallel c$ is consistent with a temperature-independent hyperfine tensor, and as shown in Fig. 3, with an absolute value of the second-order crystal-field parameter D which increases with temperature, contrary to the usual decrease found in insulators.^{13,14} The increase of $|D|$ toward high temperatures indicates that the Mn^{2+} ions are weakly coupled to the lattice vibrations, consequently the lattice thermal expansion should be responsible for the observed temperature dependence of this parameter.¹⁵ Although no thermal expansion measurements are available for $AlCl_3$ -GIC's, the temperature dependence and relative change of I_c (distance between adjacent intercalant layers) found for other GIC's (Ref. 16) in the same range of temperature are quite comparable to those found for the second-order crystal-field parameter $|D|$.

Figures 4(a) and 5(a) show, respectively, for sample No. 1 and No. 2, the temperature dependence of the resonance linewidth for one of the Mn^{2+} transitions which are not sensitive to crystal-field distortions, $\Delta M = (\frac{1}{2} \leftrightarrow -\frac{1}{2})$ and $m = \frac{5}{2}$. Up to temperatures of the order of 200 K the linewidth is temperature independent, and therefore could be taken as a lower limit for T_2 , the spin-spin relaxation time, but for $T > 200 \text{ K}$ a clear thermal

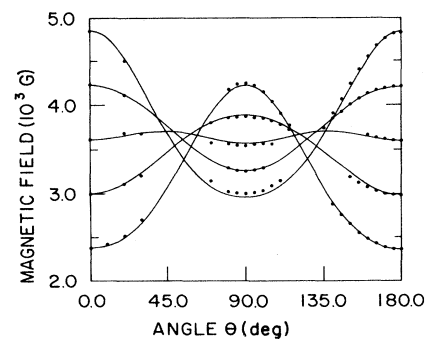


FIG. 2. Angular dependence of the Mn^{2+} transitions $|M, m = \frac{5}{2}\rangle \leftrightarrow |M-1, m = -\frac{5}{2}\rangle$ in stage-2 $AlCl_3$ -GIC. Solid lines are the best fit of Eq. (1).

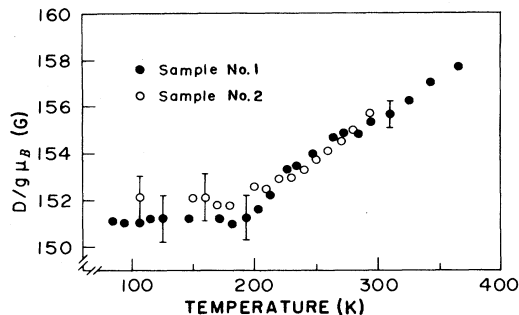


FIG. 3. Temperature dependence of the absolute value of the axial crystal-field parameter $|D(T)|$ (see text); solid circles, sample No. 1, open circles, sample No. 2.

broadening of the linewidth is observed. We believe that this is because T_1 , the spin-lattice relaxation time, becomes comparable to T_2 , and consequently T_1 can be obtained directly from the linewidth.¹⁷ Extracting the temperature dependence of the spin-lattice relaxation rate from the linewidth, $T_1^{-1} = \gamma \Delta H$, we found that the best fit of the experimental data for $T > 250$ K gives $T_1^{-1} = (11 \pm 1) \times 10^2 \times T^{(2.0 \pm 0.5)}$ and $T_1^{-1} = (4.8 \pm 0.5) \times 10^2 \times T^{(2.3 \pm 0.5)}$ for samples No. 1 and No. 2, respectively. Since the Debye temperature (θ_D) is known to be relatively small for GIC's ($200 < \theta_D < 400$ K),¹⁸ the weak temperature dependence found for the spin-lattice relaxation rate ($T_1^{-1} \propto T^2$) may be attributed to a Raman relaxation mechanism for $T > \theta_D$.¹⁹ Figures 4(b) and 5(b) show, respectively, the temperature dependence of the relative resonance intensity for the Mn^{2+} transitions and sample corresponding to Figs. 4(a) and 5(a). Although an

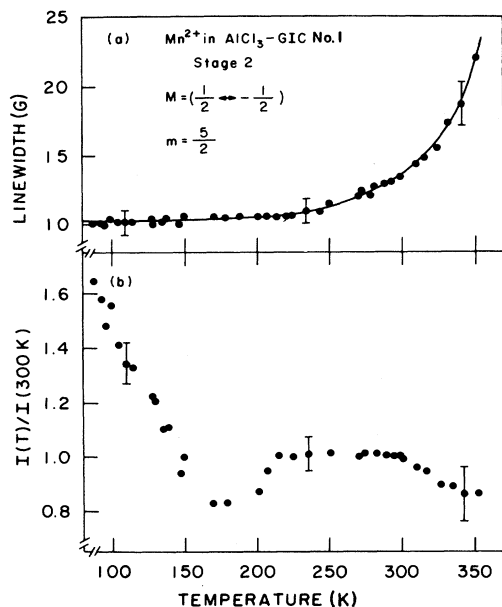


FIG. 4. Temperature dependence of the (a) linewidth and (b) relative intensity of the Mn^{2+} , $M = (\frac{1}{2} \leftrightarrow -\frac{1}{2})$, $m = \frac{5}{2}$ transition for sample No. 1 and $\mathbf{H}_0 \parallel c$.

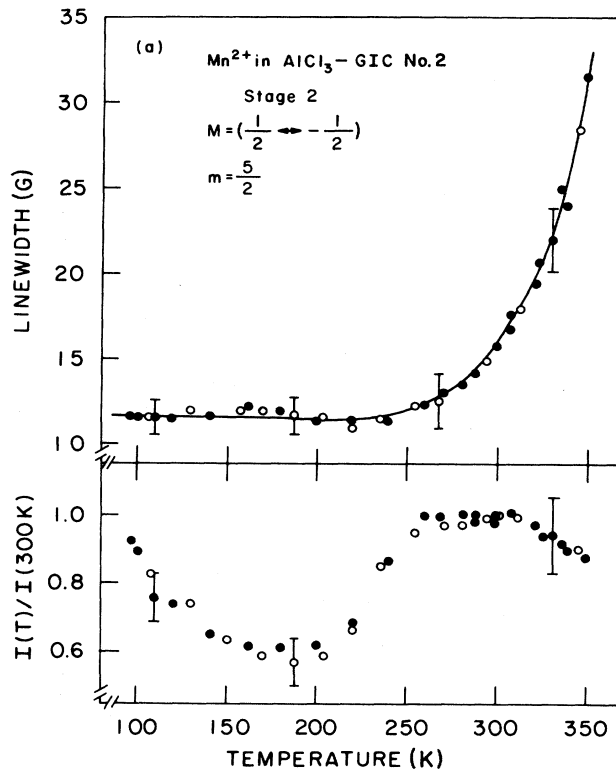


FIG. 5. Temperature dependence of the (a) linewidth and (b) relative intensity of the Mn^{2+} , $M = (\frac{1}{2} \leftrightarrow -\frac{1}{2})$, $m = \frac{5}{2}$ transition for sample No. 2 and $\mathbf{H}_0 \parallel c$. Solid and open circles correspond to decreasing and increasing temperatures, respectively.

anomalous behavior is observed at $T \approx 200$ K, which will be discussed below, and in spite of the decrease of the microwave skin depth due to the increase in the in-plane and c -axis conductivity generally found for low-stage GIC's,²⁰ the tendency of the resonance intensity is to increase toward low temperatures, indicating that the Mn^{2+} spins are localized in AlCl_3 -GIC's.

Figures 6–8 show the temperature dependence of the linewidth and relative intensity of the CCSR for samples No. 0, No. 1, and No. 2, respectively. The data were taken for the external magnetic field (\mathbf{H}_0) parallel and perpendicular to the c axis and for fast (200 K/min) and slow (1 K/min) cooling rates. Table I shows that the small anisotropy measured for the g values is temperature independent. Figures 6 and 7 show the absence of anisotropy in the linewidth and relative intensity for samples No. 0 and No. 1. These figures also show the usual decrease of the CCSR intensity toward low temperatures due to the decrease of the skin depth.²⁰ For slow cooling rates, the broadening and small hysteresis of the linewidth at $T \leq 200$ K, and the anomalies at $T \approx 200$ K in the resonance intensity, all due to an in-plane order-disorder phase transition,^{21,22} are also clearly shown. Table I and Fig. 8 show the data for sample No. 2. The main features observed in this sample are (a) the g -value anisotropy, within the accuracy of the experiment, is comparable to that of samples No. 0 and No. 1, (b) the temperature dependence of the linewidth, for slow cool-

ing rates, is roughly the same as those of samples No. 0 and No. 1, whereas for fast cooling rates and below $T \cong 200$ K, the linewidth becomes much broader and also anisotropic, and (c) the relative intensity of the resonance decreases toward low temperatures, similarly to samples No. 0 and No. 1 for fast cooling rates. For slow cooling rates the intensity was not analyzed because in this case large changes in the line shape were observed between room and low temperatures.

We should mention that, differently from the CCSR behavior, the data corresponding to the resonance of the Mn^{2+} ions were not affected by the different cooling rates.

For simplicity the line shape of the CCSR were all analyzed in terms of Dyson's theory^{23,24} in the limit of thick samples and homogeneous resonances. Therefore the values obtained for the g values and linewidth may need to be corrected because, due to the conductivity anisotropy, electromagnetic configuration, and size of the samples it is expected that in our experiments the microwave propagates mainly along the high conducting planes penetrating the sample with a skin depth governed by the c -axis resistivity.¹⁰ Thus the penetration depth along the direction of the microwave propagation will be comparable to the size of our samples, leading consequently to the intermediate, instead of the thick case in Dyson's theory. Actually we have observed some differences in the line shape of the CCSR and their temperature dependence for the three studied samples, suggesting that conductivity anisotropy effects and small differences in the size of the samples may have been responsible for the observed absorption shapes.¹⁰ On the other hand it is possible, as in $SbCl_5$ -GIC's,²⁵ that the resonances may not be homogeneous and the application of Dyson's theory may be in-

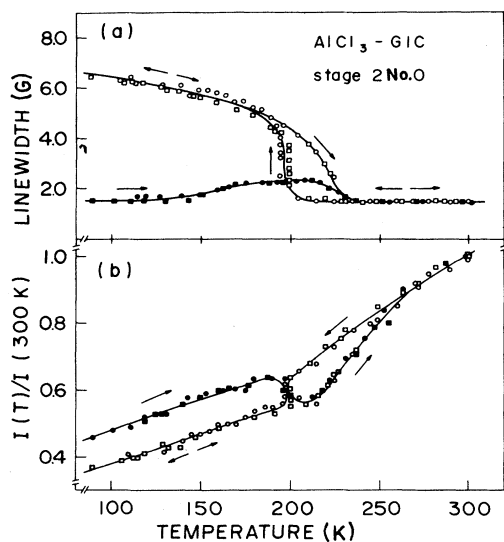


FIG. 6. Temperature dependence of the CCSR in stage-2 $AlCl_3$ -GIC, sample No. 0. (a) linewidth and (b) relative intensity. Open and solid symbols correspond to slow and fast cooling rates, respectively. Circles and square symbols correspond to $H_0 \perp c$ and $H_0 \parallel c$, respectively.

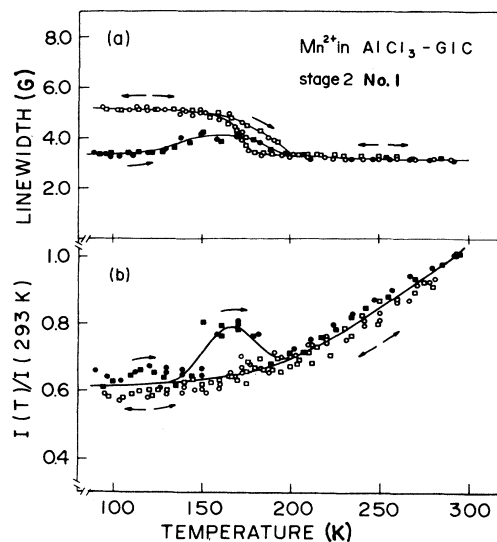


FIG. 7. Temperature dependence of the CCSR in Mn^{2+} : stage-2 $AlCl_3$ -GIC, sample No. 1. (a) linewidth and (b) relative intensity. Open and solid symbols correspond to slow and fast cooling rates, respectively. Circles and square symbols correspond to $H_0 \perp c$ and $H_0 \parallel c$, respectively.

correct. In any case the features of interest shown in this work are all too large to be simply due to line-shape effects. Therefore we believe that the application of Dyson's theory in the limit of thick samples is fairly justified.

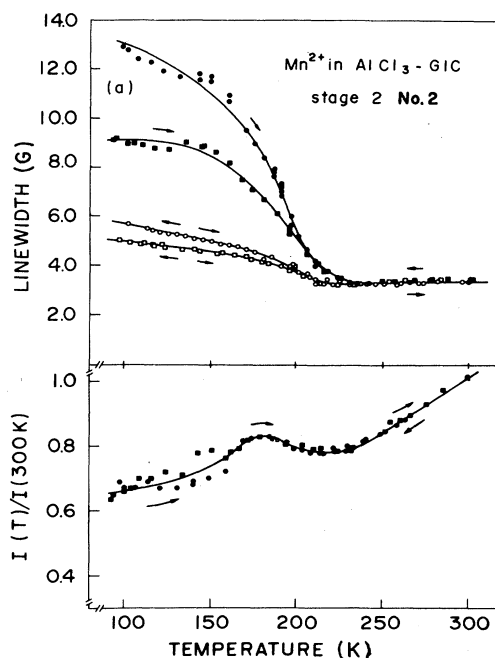


FIG. 8. Temperature dependence of the CCSR in Mn^{2+} : stage-2 $AlCl_3$ -GIC, sample No. 2. (a) linewidth and (b) relative intensity. Open and solid symbols correspond to slow and fast cooling rates, respectively. Circles and square symbols correspond to $H_0 \perp c$ and $H_0 \parallel c$, respectively.

From the anomalies observed at $T_c \cong 200$ K in our spin-resonance experiments and also in the resistivity,^{20,26} specific-heat,²⁷ and x-ray diffraction experiments,²⁸ it is evident that around this temperature there is a transition in the stage-2 AlCl_3 -GIC's. We attribute this transition to an in-plane order-disorder-type of phase transition experienced by one of the intercalant molecular species.²⁹ We suggest that above T_c these molecules are in a quasi-two-dimensional (2D) liquidlike phase, and below T_c , for a fast cooling experiment, these molecules would be frozen in a quasi-2D solidlike disordered metastable state^{21,22} of almost commensurate microdomains,²⁹ causing no effects on the linewidth of the CCSR. Except for the mobility of the molecules, this metastable state would be equivalent, as far as the conduction-carrier spin-flip scattering is concerned, to the high-temperature quasi-2D liquidlike phase. Moreover, for slow cooling rates and around T_c , similarly to other cases,^{21,22} the intercalant molecules may migrate, allowing the domains to grow in size and in turn broadening the CCSR.³⁰ On the other hand, a quite different behavior was found for sample No. 2, where fast cooling experiments lead to a much broader and also anisotropic linewidth at low temperature [see Fig. 8(a)]. We think that the higher Mn concentration in this sample, due to the longer intercalation time, makes the low-temperature structurally disordered microdomains, obtained in fast cooling experiments, to be also magnetically disordered, causing an anisotropic inhomogeneous broadening of the resonance of magnetic origin, which narrows above T_c in consequence of motional narrowing effects. Moreover, this sample shows at low temperatures and for fast cooling rates that ΔH_{\perp} is larger than ΔH_{\parallel} [see Fig. 8(a)], indicating that the high-conducting planes may also be planes of easy magnetization.

The anomaly in the temperature dependence of the relative intensity of the Mn^{2+} ($\frac{1}{2} \leftrightarrow -\frac{1}{2}$) transition observed at around 200 K [see Figs. 4(b) and 5(b)] suggests that during the domain growth the Mn^{2+} ions may migrate and form small "clusters," or regions of high Mn^{2+} concentration, which would be responsible for the observed anomalous decrease of the resonance intensity. It is interesting to note that for slow cooling rates the three samples showed approximately the same broadening of the CCSR, whereas only in the case of sample No. 2 was the line shape strongly temperature dependent. Then it seems that the formation of these small "clusters" does not affect the conduction-carrier spin-flip scattering, while for sample No. 2, a much larger number of these "clusters" may have been responsible for the observed large temperature dependence of the CCSR line shape. In any case magnetization measurements are needed to further clarify this point.

Now, except for the small broadening of the outer set of hyperfine lines observed at low temperatures, due to

probably small misorientation of the microcrystals or to a distribution of distortions along the c axis, the Mn^{2+} fine structure remains resolved at all temperatures with the symmetry axis unchanged along the c axis. This leads us to conclude that the order-disorder phase transition must preserve the orientation of the intercalant molecules along the c axis. Therefore this order-disorder phase transition should be caused by either rotational or translational molecular motions around and perpendicular to the c axis, respectively. This molecular motion may be responsible for the weak coupling of the magnetic ions to the lattice vibration suggested by the temperature dependence of $|D|$. Evidence for rotational motion at these temperatures has already been reported in heat capacity³¹ and neutron scattering³² experiments in SbCl_5 - and HNO_3 -GIC's, respectively, and translational motions in x-ray diffraction and ESR experiments in SbCl_5 - (Ref. 22) and AlCl_3 - (Ref. 30) GIC's.

Finally we should mention that in a previous work²¹ on thin samples along the c axis (thickness $\lesssim 0.1$ mm) of pure stage-2 AlCl_3 -GIC's we did not observe the order-disorder phase transition found in the present work. Although we do not have a definite explanation for that, we think that it may be related to the fact that in the present work we used thicker samples. Thick samples and large anisotropic resistivities yield the resonance to be mainly associated to the bulk of the sample¹⁰ which, being freer of defects than the surface, would lead to narrower resonances, and consequently the line broadening, due to phase transitions, to be much more easily observable.

CONCLUSIONS

In summary, we simultaneously showed for the first time in a metallic host the conduction-carrier spin resonance and the complete resolved spectra of Mn^{2+} ions. This may have been possible because there may be very small exchange coupling between the Mn^{2+} magnetic moments and the host's conduction electrons. The results indicate that the magnetic ions are sited in an axial crystal field at all temperatures and, due to the molecular mobility above $T \cong 200$ K, they are weakly coupled to the lattice vibrations. The presence of an order-disorder phase transition at $T \cong 200$ K was confirmed also for stage-2 AlCl_3 -GIC's.

ACKNOWLEDGMENTS

We are grateful to Professor A. W. Moore from Union Carbide Corporation for the HOPG and to Osram do Brasil for the quartz tubes used in this work. This work was partially supported by Fundação de Amparo Pesquisa do Estado de São Paulo (FAPESP) and Conselho Nacional de Desenvolvimento Científico e Tecnológico (CNPq), Brazil.

¹G. Wagoner, Phys. Rev. **118**, 647 (1960).

²P. Lauginie, H. Estrade, J. Conard, D. Guerard, P. Lagrange, and M. El Makrini, Physica B+C **99B**, 514 (1980).

³S. K. Khana, E. R. Falardeau, A. J. Heeger, and J. F. Fischer,

Solid State Commun. **25**, 1059 (1978).

⁴R. M. Stein, L. Walmsley, G. M. Gualberto, and C. Rettori, Phys. Rev. B **32**, 4774 (1985).

⁵K. A. Müller and R. Kleiner, Phys. Lett. **1**, 98 (1962).

- ⁶K. Koga, M. Suzuki, and H. Yasuoka, *Synth. Metals* **12**, 467 (1985).
- ⁷M. Suzuki and H. Suematsu, *Synth. Metals* **6**, 173 (1983).
- ⁸D. Vaknin, D. Davidov, H. Selig, and Y. Yeshurun, *J. Chem. Phys.* **83**, 3859 (1985).
- ⁹D. Vaknin, D. Davidov, H. Selig, V. Zevin, I. Felner, and Y. Yeshurun, *Phys. Rev. B* **31**, 3212 (1985).
- ¹⁰L. Walmsley, G. Ceotto, J. H. Castilho, and C. Rettori, *Synth. Metals* (to be published).
- ¹¹G. M. Gualberto, C. Underhill, S. Y. Leung, and G. Dresselhaus, *Phys. Rev. B* **21**, 862 (1980).
- ¹²C. F. Hempstead and K. D. Bowers, *Phys. Rev.* **118**, 131 (1960).
- ¹³R. A. Serway, *Phys. Rev. B* **3**, 608 (1971).
- ¹⁴F. J. Owens, *Phys. Rev. B* **10**, 78 (1974).
- ¹⁵D. F. Wait, *Phys. Rev.* **132**, 601 (1963).
- ¹⁶F. McRae, J. F. Mareché, A. Bendriss-Rerhaye, P. Lagrange, and M. Lelavrain, *Ann. Phys. (Paris) Colloq.* **11**, 13 (1986).
- ¹⁷A. A. Manenkov and V. A. Milyaev, *Zh. Eksp. Teor. Fiz.* **41**, 100 (1962) [*Sov. Phys.—JETP* **14**, 75 (1962)].
- ¹⁸M. S. Dresselhaus and G. Dresselhaus, *Adv. Phys.* **30**, 139 (1981).
- ¹⁹J. A. Van Vleck, *Phys. Rev.* **57**, 426 (1940).
- ²⁰E. McRae and J. F. Mareché, *J. Mater. Res.* (to be published).
- ²¹R. M. Stein, L. Walmsley, and C. Rettori, *Phys. Rev. B* **32**, 4134 (1985).
- ²²S. Rolla, L. Walmsley, H. Suematsu, C. Rettori, and Y. Yosida, *Phys. Rev. B* **36**, 2893 (1987).
- ²³F. J. Dyson, *Phys. Rev.* **98**, 349 (1955).
- ²⁴G. Feher and A. F. Kip, *Phys. Rev.* **98**, 337 (1955).
- ²⁵S. Rolla, Ph.D. thesis, UNICAMP, Campinas (SP) Brazil, 1989.
- ²⁶B. Bach and A. R. Ubbelohde, *Proc. R. Soc. London, Ser. A* **325**, 437 (1971).
- ²⁷A. Baiker, E. Habberger, U. K. Sharma, and W. Richarz, *Carbon* **19**, 327 (1981).
- ²⁸R. Vangelisti and M. Lelaurain, *Carbon* **24**, 654 (1986).
- ²⁹P. Behrens, U. Weigand, and W. Metz (unpublished).
- ³⁰R. M. Stein, L. Walmsley, S. Rolla, and C. Rettori, *Phys. Rev. B* **33**, 6524 (1986).
- ³¹D. N. Bitner and M. Bretz, *Phys. Rev. B* **31**, 1060 (1985).
- ³²F. Batallan, I. Rosenman, A. Margerl, and H. Fuzellier, *Phys. Rev. B* **32**, 4810 (1985).